Available online at www.sciencedirect.com
ScienceDirect
International Journal of Heat and Mass Transfer 50 (2007) 5073–5086
International Journal of HEAT and MASS TRANSFER
www.elsevier.com/locate/ijhmt

Evaporation of acoustically levitated multi-component liquid droplets

G. Brenn [a,*], L.J. Deviprasath [b], F. Durst [b], C. Fink [c]

[a] Institute of Fluid Mechanics and Heat Transfer, Graz University of Technology, Inffeldgasse 25/F, 8010 Graz, Austria
[b] Institute of Chemical and Bioengineering, LSTM, University of Erlangen-Nürnberg, Cauerstrasse 4, 91058 Erlangen, Germany
[c] Competence Centre "The Virtual Vehicle", Inffeldgasse 21A, 8010 Graz, Austria

Received 2 March 2007
Available online 21 September 2007

Abstract

A theoretical model for the evaporation of multi-component liquid droplets based on the model by Abramzon and Sirignano is presented and applied to the evaporation of acoustically levitated droplets. The liquid phase is treated as a thermodynamically real fluid, using the UNIFAC method for calculating the component activities, and the gas phase as ideal. Computational results, which consist in the droplet surface and volume, temperature and composition as functions of time, are verified by experiments carried out with single droplets evaporating in an acoustic levitator. The results are in excellent agreement, suggesting that the model correctly captures the physico-chemical phenomena in multi-component liquid droplet evaporation.

Keywords: Droplet; Evaporation; Multi-component mixture; Acoustic levitation; UNIFAC model

1. Introduction

The evaporation of liquid droplets into a gaseous environment is a process extensively employed in process engineering and in energy conversion and has therefore been of great interest to engineers since decades. Because of this, numerous investigations have been performed to study the evaporation of liquid droplets with different thermodynamic properties. For pure liquids it appears that the theory has been sufficiently developed to predict not only the droplet diameter – or volume – variation with time, but also the variation of the thermodynamic state of the droplet liquid during the evaporation process. Hence, the theory for pure liquids can be used successfully to lay out equipment employed in technical processes.

In many applications, however, the evaporating liquid droplets contain many components with different thermodynamic properties. In the last few decades, extensive research has been carried out on the problem of multi-component liquid droplet evaporation. Newbold and Amundson [1] described the evaporation behaviour of droplets of binary and ternary mixtures. These authors found that the augmentation of the diffusive mass transport by the Stefan flow from the droplet surface, as described by Frank-Kamenetzki [2], plays an essential role in their model predictions. Their work also demonstrated that an augmentation of the transport of one component by the presence of the other may occur. Abraham and Magi [3] developed a model of multi-component droplet evaporation in sprays, highlighting the importance of the volatility of the components for the evaporation and also the inter-species liquid diffusivity. Law and Law [4] pointed out the existence of a multi-component analog of the classical d^2-law of droplet evaporation in the case that the slow rate of liquid phase diffusion is taken into account. This effect causes the droplet concentration distributions to remain almost constant during much of the droplet lifetime. Kneer et al. [5] examined the importance of variable liquid properties in droplet evaporation. Their computations show the presence of large temperature and concentration gradients inside the droplet, which cause variations in the physico-chemical properties during the evaporation. Their work also emphasised the need to account for the non-ideal

* Corresponding author. Tel.: +43 316 873 7341; fax: +43 316 873 7356.
E-mail address: brenn@fluidmech.tu-graz.ac.at (G. Brenn).

0017-9310/$ - see front matter © 2007 Elsevier Ltd. All rights reserved.
doi:10.1016/j.ijheatmasstransfer.2007.07.036

Nomenclature

a	drop radius (m)
B_M	Spalding mass transfer number
B_T	Spalding heat transfer number
Ba	acoustic Bond number
Bo	Bond number
c	sound speed (m/s)
c_p	specific isobar heat capacity (J/(kg K))
d	drop diameter (m)
D	diffusion coefficient (m^2/s)
Fo	Fourier number
g	gravitational acceleration (m/s^2)
k	wave number (1/m)
L	latent heat of evaporation (J/kg)
Le	Lewis number
$m, \dot{m}$	mass, evaporation rate (kg, kg/s)
N	number of components
Nu, Nu^*	usual and modified Nusselt number
p	pressure (N/m^2)
Pr	Prandtl number
Q_L	heat transfer rate into the liquid (W)
Re	Reynolds number
Sc	Schmidt number
Sh, Sh^*	usual and modified Sherwood number
t	time (s)
T	temperature (K)
U	velocity (m/s)
v	velocity (m/s)
V	volume (m^3)
x	mole fraction of mixture component
Y	mass fraction of mixture component

Greek symbols

β	aspect ratio
γ	activity coefficient
κ	non-dimensional wave number
λ	wavelength (m)
Λ	Wilson coefficient
μ	dynamic viscosity (kg/(m s))
ρ	density (kg/m^3)
σ	surface tension (N/m)
ϕ	exponent; levitation safety factor
φ	volume fraction

Subscripts

0	small transfer rate; initial state
2	binary mixture
∞	state of host medium
A, B	components
d	droplet
eff	effective
F	fuel
g	gaseous phase
i	mixture component
L	liquid
m	mixture
max	maximum
min	minimum
S	surface
vap	vapour

behaviour of both the liquid and the gas phases in order to match the real conditions, and the importance of variable physical properties in the calculation of the droplet evaporation rate.

The above cited work shows that, in general, there is no way to utilise average thermodynamic properties of a multi-component liquid for predicting droplet evaporation on the basis of the theory for pure liquids. A more detailed analysis is necessary to model the contributions from each component to the evaporation and to take interactions between the liquid components into account for predicting the evaporation of multi-component liquid droplets into their gaseous environment accurately. Marchese and Dryer presented a detailed analysis of the evaporation of methanol–water mixture droplets solving the full set of equations of change numerically, but in a spatially one-dimensional approximation [6]. In their work they used the Wilson coefficients approach to account for the influence of the composition of the liquid mixture on the vapour pressures of the two components. Many other investigations in the existing literature, however, rely on Raoult's law for calculating the vapour pressures of the liquid components. It is the objective of the present study to present a more realistic model for describing the physico-chemical behaviour of evaporating multi-component liquid droplets, which accounts for the real liquid mixture behaviour by calculating the activities of the components, rather than incorporating Raoult's law. The simplification in using Raoult's law consists in the assumption that the mole fractions of the mixture components are close to one, which is mostly not correct for all components in a multi-component liquid. The resulting equations for the vapour pressures of the components are very simple linear relationships between vapour pressure of the pure component and the mole fraction of the component in the liquid phase. The drawback, however, is considerable inaccuracy in the calculation of the vapour pressures, which may be unacceptable for many simulations of technical processes with liquid evaporation. The model presented is based on the well accepted evaporation model by Abramzon and Sirignano, which was developed for pure liquids [7] and is extended here to the multi-component case. This model includes the effect of the Stefan flow on the heat and mass transfer, and it describes the evaporation process even at

high transfer rates by making use of the film theory for calculating the Nusselt and Sherwood numbers [8].

The following section of our paper presents the mathematical model for describing liquid droplet evaporation and the physico-chemical behaviour of multi-component liquids. Thereafter we present the experimental technique used for validating the model predictions by measuring the evaporation behaviour of single droplets of multi-component liquids. In Section 4 we present the validation of the model against experimental data. Section 5 presents a further series of advanced experimental and computational results, together with a discussion. The paper ends with the conclusions.

2. Mathematical modelling

For developing a thorough description of the evaporation of multi-component liquid droplets, a realistic model for describing the heat and mass transport processes across the liquid/gas interface is needed together with an approach to account for the effects of the multi-component liquid composition on the physico-chemical properties relevant for the evaporation of all the components. For describing the transport processes, the present work is based on the droplet evaporation model developed by Abramzon and Sirignano [7]. This is a widely accepted and applied approach, which predicts the evaporation rate and droplet heating more accurately than other theories, which do not account for the effects of high transfer rates on the transfer coefficients. The model was extended by Kastner to binary liquid mixtures, accounting for the relevant physico-chemical properties of the real binary liquid mixtures by the Wilson coefficients approach [9]. Kneer presented an extension of the model to multi-component liquids, but did not give details on the calculation of the component activities [10]. The present work formulates an alternative extension of the model to multi-component liquid droplets, using the UNIFAC approach for calculating the vapour pressures of the various mixture components.

2.1. The model by Abramzon and Sirignano

In the model by Abramzon and Sirignano for the evaporation of a liquid droplet, it is assumed that

1. the droplet is spherical all the time,
2. the solubility of air in the liquid is negligible,
3. mass diffusion due to temperature and pressure gradients is negligible,
4. the gas phase is in a quasi-steady state,
5. the droplet evaporates in an inert environment without chemical reactions, and that
6. heat transfer due to radiation is negligible.

The gas flow relative to an evaporating droplet with a velocity U is in principle unsteady due to the temporal evolution of the droplet size d. A characteristic time for the flow in the gas phase is $O(d/U)$, which is in all practical cases much smaller than the lifetime of the droplet. Hence, the assumption that the gas phase is at a quasi-steady state is justified. The model accounts for the Stefan flow in the gas phase and describes the transfer rates by modified Nusselt and Sherwood numbers. An infinite conductivity and rapid mixing model was used for modelling the liquid phase temperature and mixture composition, which are then both spatially constant in the droplet during the evaporation process. The Fourier and Fickian laws are used to describe the conductive heat and diffusional mass transfer, respectively, in the gas phase. With the approach of the film theory, Abramzon and Sirignano obtained the evaporation rate of a pure liquid droplet as

$$\dot{m} = 2\pi a(\bar{\rho}\overline{D})_{\mathrm{g}} Sh^{*} \ln(1 + B_M), \tag{1}$$

where a is the time-dependent radius of the droplet, $\bar{\rho}_{\mathrm{g}}$ and $\overline{D}_{\mathrm{g}}$ are the mean density of the gas phase and the mean binary diffusion coefficient of the vapour in the gas film, Sh^{*} is a modified Sherwood number, and B_M the Spalding mass transfer number. The modified Sherwood number accounts for the effect of a high mass transfer rate and is defined by the equation

$$Sh^{*} = 2 + \frac{Sh_0 - 2}{F(B_M)} \tag{2}$$

with the Sherwood number Sh_0 for small mass transfer rate given by the Frössling correlation [11]

$$Sh_0 = 2 + 0.552 Re^{1/2} Sc^{1/3} \tag{3}$$

or a similar correlation found by Ranz and Marshall [12]. The function $F(B)$ reads

$$F(B) = (1 + B)^{0.7} \frac{\ln(1 + B)}{B}. \tag{4}$$

The symbol B may represent the Spalding mass transfer number B_M, as it is the case in Eq. (2). This number is given by the equation

$$B_M = \frac{Y_{\mathrm{F,S}} - Y_{\mathrm{F},\infty}}{1 - Y_{\mathrm{F,S}}}, \tag{5}$$

where $Y_{\mathrm{F,S}}$ and $Y_{\mathrm{F},\infty}$ are the mass fractions of the liquid (“fuel”) vapour at the droplet surface and in the undisturbed ambient medium, respectively. In describing the heat transfer, B represents the Spalding heat transfer number B_T, which will be introduced below. In Eq. (3), Re and Sc are the Reynolds number of the flow around the droplet and the Schmidt number of the gaseous phase, respectively. In the present context, the Reynolds number is calculated with an effective velocity of the acoustic streaming in the levitator, where the droplets are placed in the experiments. Acoustic streaming is a time-independent secondary flow induced by the presence of the droplet as an obstacle in the otherwise periodic acoustic boundary-layer flow. This secondary flow has a convective influence on the droplet, which is equivalent to the effects of a flow around the

droplet in translatory motion [13]. A procedure developed by Lierke is used to calculate the effective velocity, which is fairly constant during the droplet evaporation process and represents this convective influence of the acoustic streaming [14]. This velocity is calculated as follows: First the acoustic force acting on the levitated droplet is calculated by integrating the sound pressure over the droplet surface. The sound pressure is taken to depend on the axial position z in the levitator by the cosine function $\cos kz$ (with the wave number k of the acoustic field). The result is an acoustic force acting on the droplet, which depends on the position of the droplet in the sound field and the oscillation velocity amplitude $v_{\max}$ of the sound field. The latter is a measure for the sound pressure level. In that integration, the function

$$f_2(\kappa) = \frac{2.29}{\kappa}\left(\frac{\sin\kappa}{\kappa} - \cos\kappa\right) \tag{6}$$

appears, where κ is the non-dimensional wave number of the sound wave. We then introduce an acoustic Bond number $Ba = \rho_g/2 \cdot v_{\max}^2/p_\sigma = \rho_g/8 \cdot v_{\max}^2 d_0^2/\sigma$, with the capillary pressure p_σ, and the Bond number $Bo = \rho_d g d_0^2/4\sigma$. Defining a"levitation safety factor" ϕ as the ratio of the maximum available acoustic force in the levitator (determined from the result of the pressure integration) and the weight of the droplet, so that

$$\phi = \frac{F_{ac,\max}}{\rho_d V_d g}, \tag{7}$$

the square of the oscillation velocity amplitude $v_{\max}$ may be calculated as

$$v_{\max}^2 = \frac{1.22\phi\rho_d g d_0}{f_2(\kappa)\rho_g}. \tag{8}$$

At the same time, from the definition of the acoustic Bond number, which also contains the velocity $v_{\max}$, it follows that it may be expressed as $Ba = 0.61\phi Bo/f_2(\kappa)$, so that the oscillation velocity amplitude is finally given by the equation

$$v_{\max} = \sqrt{\frac{4.88Bo\phi\sigma}{f_2(\kappa)\rho_g d_0}}. \tag{9}$$

In this equation the Bond number still appears. For this quantity, Marston et al. [15] found that, in the case of small values of the factor ϕ, its value is given as

$$Bo = \frac{\left[\beta_{\min}^{1/3} - 1\right] f_2(\kappa)}{0.02288[5 + 1.75(kd_0)^2]}, \tag{10}$$

where β is the aspect ratio of the spheroidal droplet shape caused by the acoustic pressure. The subscript min denotes the value of this ratio at values of the factor ϕ close to one, which is the minimum required level for levitating the droplet. The analysis of Marston et al. evaluates the sound pressure field in the standing wave and determines the static deformation of the droplet influenced by the pressure distribution in space. With the given oscillation velocity amplitude $v_{\max}$ in the sound field, the effective velocity of the acoustic streaming now follows from the equation:

$$v_{\text{eff}} = \frac{2}{kd_0}\frac{v_{\max}^2}{c} \tag{11}$$

with the wave number $k = 2\pi f/c$ of the acoustic field, the initial equivalent droplet diameter d_0, the sound speed c in the ambient gas, and the sound frequency f. This equation is given by Gopinath and Mills in their work [16] and originates from an analysis of the acoustically induced secondary flow around the drop. With v_{eff} we calculate the Reynolds number Re as

$$Re = \frac{v_{\text{eff}} d_0 \rho_g}{\mu_g} \tag{12}$$

with the dynamic viscosity μ_g of the ambient medium.

The transfer of heat from the ambient medium to the liquid droplet provides the energy needed for the evaporation taking place at the wet-bulb temperature of the liquid in the ambient medium at the given thermodynamic state. For quantifying this heat transfer rate, the evaporation rate of the liquid droplet is calculated in two ways, as given in detail in [7]. First, the evaporation rate is expressed as dependent on the Sherwood number, calculating the rate of transport of mass in the Stefan flow. Second, it is expressed as dependent on the Nusselt number, calculating the rates of heat transport through a control shell on the surface of the droplet. Equating the two expressions obtained to eliminate the evaporation rate yields the rate Q_L of heat transported from the ambient air into the liquid as

$$Q_L = \dot{m}\left[\frac{\bar{c}_{p,F}(T_\infty - T_S)}{B_T} - L(T_S)\right]. \tag{13}$$

Here $L(T_S)$ is the latent heat of evaporation of the liquid at the droplet surface temperature T_S, and $B_T = (1 + B_M)^\phi - 1$ is the Spalding heat transfer number already mentioned above [7]. The exponent ϕ is given as

$$\phi = \frac{\bar{c}_{p,F}}{\bar{c}_{p,g}}\frac{Sh^*}{Nu^*}\frac{1}{\overline{Le}}. \tag{14}$$

The bars on the specific heat capacities c_p indicate average values between the thermodynamic states at the droplet surface and in the ambient gas. $\overline{Le}$ is the average Lewis number of the gas mixture. The modified Nusselt number Nu^* is given by an equation analogous to Eq. (2), with B_M replaced by B_T and Sh_0 replaced by $Nu_0 = 2 + 0.552Re^{1/2}Pr^{1/3}$. The rate of change of the droplet temperature T_S for the infinite conductivity (or lumped-capacity) approach is determined by the equation

$$\frac{dT_S}{dt} = \frac{3}{4\pi a^3 \rho_L c_{p,L}} Q_L, \tag{15}$$

which is used for determining the droplet temperature as a function of time. We use this approach here since the

acoustically levitated drops we investigate are well mixed by the interaction with the acoustic streaming and therefore exhibit flat temperature profiles, which is a situation equivalent to a small Biot number of heat transfer.

In cases where mixing processes inside the droplet are absent, the temperature (and component concentration) profiles inside the droplet must be computed by solving the related transport equations for the droplet. This has been done by Marchese and Dryer in a detailed study, who solved the set of continuity, component mass balance, and thermal energy equations for both the liquid and the gas phases to simulate the evaporation of methanol/water binary mixture drops in air [6]. They deduced information about the temporal evolutions of the drop diameter squared, the drop surface temperature, and component mass fractions, to name but a few. For the present problem, we do not need to solve the transport equations, for the above named reasons. In terms of composition of the liquid phase, we go to larger numbers of components than [6] and present a model that allows for the computation of their activities.

2.2. Extension of the model to multi-component liquids

It is one purpose of the present work to extend the above model to enable the computation of the evaporation of multi-component liquid droplets. In this extended model we formulate the evaporation rate of the droplet as the sum of all component evaporation rates, i.e., by an equation of the form

$$\dot{m} = \sum_{i=1}^{N} \dot{m}_i = 2\pi \sum_{i=1}^{N} a_{V,i} (\bar{\rho}\overline{D}_i)_{\mathrm{g}} Sh_i^* \ln(1 + B_{M,i}) \tag{16}$$

for an N-component mixture, where $\dot{m}_i$ is the evaporation rate of the liquid component i in the droplet. In the above equation, $a_{V,i}$ is the volume equivalent partial radius of component i corresponding to its instantaneous volume fraction φ_i in the liquid mixture. This partial radius, which is defined as $a_{V,i} = a\varphi_i^{1/3}$, was found to be the right length scale to represent the evaporation rates of the mixture components in multi-component liquid droplets evaporation [17]. The quantity $\overline{D}_i$ is the mean diffusion coefficient of the vapour of component i in dry air. The modified Sherwood number Sh_i^* is calculated individually for each component i, using the component vapour properties and the drop diameter $d = 2a$ as the length scale of the Re number. The Spalding mass transfer number $B_{M,i}$ is computed for each component i according to

$$B_{M,i} = \frac{Y_{i,\mathrm{S}} - Y_{i,\infty}}{1 - Y_{i,\mathrm{S}}} \tag{17}$$

The other symbols in Eq. (16) have their usual meanings. The diffusion coefficient of component i is still a binary coefficient, since we consider the gas phase as ideal and therefore ignore effects from vapour components other than i in the gas phase.

The rate of heat transfer into the liquid is modelled by an equation analogous to Eq. (13) for all components separately, which reads

$$Q_{\mathrm{L}} = \sum_{i=1}^{N} \dot{m}_i \left[\frac{\bar{c}_{p,i}(T_\infty - T_{\mathrm{S}})}{B_{T,i}} - L_i(T_{\mathrm{S}}) \right] \tag{18}$$

This means that the liquid mixing enthalpy is not accounted for and therefore the liquid mixture is treated as ideal in the caloric sense. It should be pointed out that, for our simulation, we assume a homogeneous liquid mixture with constant component mass fractions throughout the droplet. This assumption is well motivated by the mixing process in the droplet mentioned above. This approach does not mean any limitation to the model for the physico-chemical behaviour of the liquid mixtures. Our approach could be equally well applied to situations with concentration profiles in our drops [18]. In our computations, the rate of change of the droplet temperature is given by the relation

$$\frac{\mathrm{d}T_{\mathrm{S}}}{\mathrm{d}t} = \frac{Q_{\mathrm{L}}}{m_{\mathrm{d}} \sum_{i=1}^{N} Y_{i,\mathrm{L}} c_{p,i,\mathrm{L}}}, \tag{19}$$

where Q_{L} is calculated using Eq. (18).

2.3. Modelling the component activities in liquid mixtures – the Wilson coefficients and UNIFAC approaches

For evaluating the above model equations, the liquid mixture is treated as real by accounting for mutual influences of the liquid components on their activities. This behaviour has consequences for the actual vapour pressures (and therefore mass fractions) of the various components in the gas phase, which is saturated at the droplet surface. The mass fractions of the components occur in the Spalding mass transfer number $B_{M,i}$, and they are needed for calculating all gas/vapour mixture properties using the 1/3-rule for defining a reference composition [7]. The mass fraction Y_i is computed from the mole fraction x_i, which is calculated as

$$x_i = \frac{p_{\mathrm{vap},i}}{p_{\mathrm{m}}} \gamma_i x_{\mathrm{L},i}. \tag{20}$$

Here $p_{\mathrm{vap},i}$ is the vapour pressure of the pure component i, γ_i is the activity coefficient of the component in the multi-component liquid mixture, and $x_{\mathrm{L},i}$ the mole fraction of component i in the liquid phase. The whole mixture equilibrium is established under the total mixture pressure p_{m}, which is the ambient atmospheric pressure, composed of the contributions from the vapour pressures of the evaporating liquids and the partial pressures of the air and the water vapour content due to the humidity of the air. An important step in the calculations is the determination of the activity coefficients γ_i. They may be calculated as follows.

In cases that the liquid is a binary mixture, the activity coefficients of the two components may be described using the Wilson coefficients [19,20]. The activity coefficients $\gamma_{2,A}$

and $\gamma_{2,B}$ of the components A and B of a binary mixture (indicated by the subscript 2) follow from the equations:

$$\ln\gamma_{2,A} = -\ln(x_{\mathrm{L},A} + \Lambda_{AB}x_{\mathrm{L},B}) + x_{\mathrm{L},B}\left[\frac{\Lambda_{AB}}{x_{\mathrm{L},A}+\Lambda_{AB}x_{\mathrm{L},B}} - \frac{\Lambda_{BA}}{\Lambda_{BA}x_{\mathrm{L},A}+x_{\mathrm{L},B}}\right] \quad (21)$$

$$\ln\gamma_{2,B} = -\ln(x_{\mathrm{L},B} + \Lambda_{BA}x_{\mathrm{L},A}) - x_{\mathrm{L},A}\left[\frac{\Lambda_{AB}}{x_{\mathrm{L},A}+\Lambda_{AB}x_{\mathrm{L},B}} - \frac{\Lambda_{BA}}{\Lambda_{BA}x_{\mathrm{L},A}+x_{\mathrm{L},B}}\right] \quad (22)$$

where $x_{\mathrm{L},A}$ and $x_{\mathrm{L},B}$ are the mole fractions of the two components in the liquid phase, and Λ_{AB} and Λ_{BA} are the Wilson coefficients.

In the case of multi-component mixtures, a different approach for calculating the component activity coefficients is needed. In our model, we use the UNIFAC method [21], a group contribution method which allows the activity coefficients of components of polynary liquid mixtures to be calculated as functions of mixture composition and temperature. UNIFAC is a combination of the UNIQUAC method with the increment method [19,22]. The increment method assumes that γ_i is composed of a combinatoric part (C) and a rest part (R). The combinatoric part stands for a contribution of the excess entropy, and the rest part for the effect of the excess enthalpy. The excess entropy is caused by the various shapes and sizes of the molecules, whereas the excess enthalpy arises from the energetic interaction between them. Thus γ_i is computed as

$$\ln\gamma_i = \ln\gamma_i^C + \ln\gamma_i^R. \quad (23)$$

The combinatoric part is calculated by the so-called UNIQUAC method as

$$\ln\gamma_i^C = \ln\frac{\psi_i}{x_{\mathrm{L},i}} + 5q_i\ln\frac{\vartheta_i}{\psi_i} + l_i - \frac{\psi_i}{x_{\mathrm{L},i}}\sum_{j=1}^{N} x_{\mathrm{L},j}l_j \quad (24)$$

with

$$l_i = 5(r_i - q_i) - (r_i - 1),$$
$$\vartheta_i = \frac{q_i x_{\mathrm{L},i}}{\sum_{j=1}^{N} q_j x_{\mathrm{L},j}}, \quad \psi_i = \frac{r_i x_{\mathrm{L},i}}{\sum_{j=1}^{N} r_j x_{\mathrm{L},j}}. \quad (25)$$

Here $x_{\mathrm{L},i}$ is the mole fraction of component i and N the number of components in the liquid mixture. r_i and q_i are the relative Van-der-Waals volume and surface, respectively. They are calculated by

$$r_i = \sum_{k=1}^{M} v_k^{(i)} R_k \quad \text{and} \quad q_i = \sum_{k=1}^{M} v_k^{(i)} Q_k, \quad (26)$$

where $v_k^{(i)}$ is the number of structure groups of type k in the molecule i. E.g., for n-pentane C_5H_{12} with its well known molecular structure, $v_1^{(i)} = 2$ ($2CH_3$-groups) and $v_2^{(i)} = 3$ ($3CH_2$-groups). M is the number of different groups in molecule i, and R_k and Q_k are constants specific for group k given in databases [19,23]. The rest part is calculated as the sum of the various group contributions:

$$\ln\gamma_i^R = \sum_{k=1}^{M} v_k^{(i)}[\ln\Gamma_k - \ln\Gamma_k^{(i)}] \quad (27)$$

Γ_k and $\Gamma_k^{(i)}$ are the group activity coefficients of group k in the mixture and in the pure liquid i, respectively. They are computed as

$$\ln\Gamma_k = Q_k\left[1 - \ln\left(\sum_{m=1}^{M}\vartheta_m\chi_{mk}\right) - \sum_{m=1}^{M}\frac{\vartheta_m\chi_{km}}{\sum_{n=1}^{M}\vartheta_n\chi_{nm}}\right] \quad (28)$$

with

$$\vartheta_m = \frac{Q_m X_m}{\sum_{n=1}^{M} X_n}, \quad X_m = \frac{\sum_{j=1}^{N} v_m^{(j)} x_j}{\sum_{j=1}^{M}\sum_{n=1}^{M} v_n^{(j)} x_j}, \quad \chi_{nm} = e^{-a_{nm}/T}. \quad (29)$$

Here a_{nm} is the group interaction parameter between groups n and m, which is available for many group combinations [22]. T is the temperature under which the vapour–liquid equilibrium is established. For the pure liquid

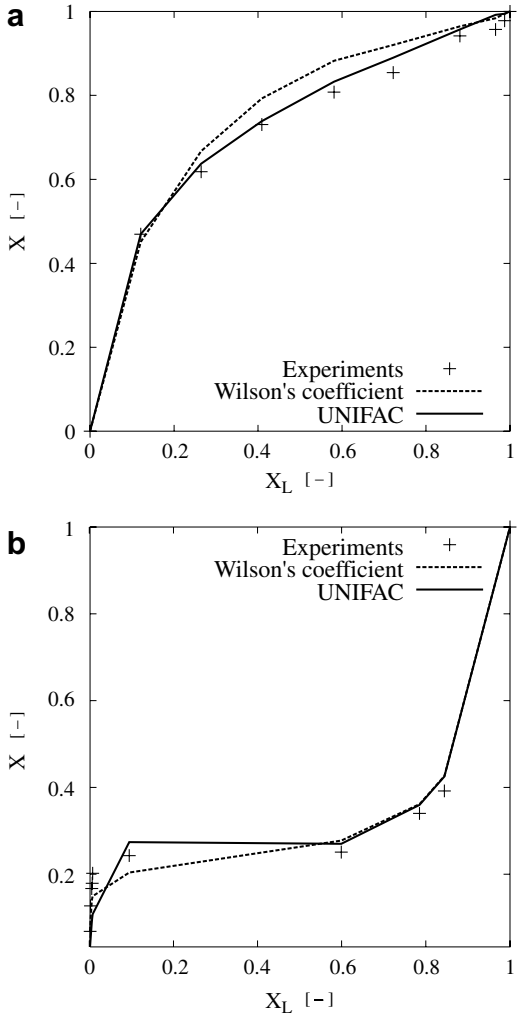

Fig. 1. Equilibrium molar fractions x of the hydrocarbon components in the vapour phase of (a) methanol–water, and (b) 1-butanol–water mixtures as functions of the molar fraction x_{L} of the component in the liquid phase. Experimental data from [24].

parameters $\Gamma_k^{(i)}$, $a_{nm} = 0$, so that $\chi_{nm} = 1$. The UNIFAC method can be applied to mixtures of an arbitrary number of components. It works for non-electrolyte, non-polymeric mixtures at low to moderate pressures and at temperatures between 300 K and 425 K [21].

Examples of molar fractions of hydrocarbon components of two selected binary mixtures in the vapour phase as functions of the liquid composition, as obtained from Wilson's coefficients and with the UNIFAC method, are shown in Fig. 1a and b in comparison with experimental data from [24]. These data show that the UNIFAC method represents the measurement data very well. Similar comparisons for multi-component mixtures are more difficult to make, since experimental data are sparse.

For the calculations in our work we use a version of a UNIFAC software available from the report [25].

3. Experimental procedure

Experiments on the evaporation behaviour of single droplets of multi-component liquids were carried out using an acoustic levitator to validate theoretical descriptions of pure liquid droplet evaporation [13,26]. Acoustic levitation is a useful experimental technique for analyzing the evaporation kinetics of single droplets. The experimental value of a levitator is that it suspends droplets without any mechanical contact by making use of the quasi-steady sound-pressure distribution in a confined space. This also helps in maintaining the thermodynamic properties of the levitated droplet and ensures that the heat transfer to an evaporating droplet is only due to the presence of an ambient gaseous medium.

Due to these advantages, an acoustic levitator is useful for tracking the life history of an evaporating droplet. Applications of acoustic levitators are manifold; apart from investigations in the fields of fluid mechanics and heat and mass transfer, the levitator is also used in various fields of material sciences (studies on melting and solidification processes, containerless processing of materials, nucleation in melts), bio-sciences (particularly for the analysis of single cells [27,28]), and bio-medical investigations (studies of cell cultures and on growth of protein crystals).

In the present study, an acoustic levitator supplied by *Battelle*, *Frankfurt* (*Germany*) was used to carry out the experiments. The experimental setup with the levitator is depicted in Fig. 2. The essential component of the levitator is an acoustic resonator consisting of a transducer and a reflector to produce standing ultrasound waves. The transducer is a stainless steel horn, which is excited to vibrate by a piezo-crystal driven by an electrical signal. The electrical signal is constantly produced at a maximum power output of 10 W. Due to the vibration, the horn emits sound waves at the vibration frequency, which in the present case is 56 kHz. The wave length λ of the sound corresponding to the unperturbed sound velocity in air of 343.8 m/s at a temperature of 293.15 K is $\lambda \approx 6.14$ mm.

The ultrasonic waves produced are made to stand by a flat reflector positioned opposite to the transducer. The standing wave produces a quasi-steady pressure distribution in the resonator, exhibiting pressure nodes and antinodes. The reflector is located at a distance appropriate to allow for the formation of five pressure nodes. In setting up the acoustic levitator, it was ensured that both the stainless steel horn and the reflector were aligned along the axis of symmetry of the levitator.

The acoustic levitator was placed in an acrylic glass box, where a controlled temperature of about 302.15 K $\pm$ 2 K and a relative humidity of 0.02 or 0.03 $\pm$ 5% were maintained throughout the experiments. In the present context, the term "relative humidity" denotes the water vapour

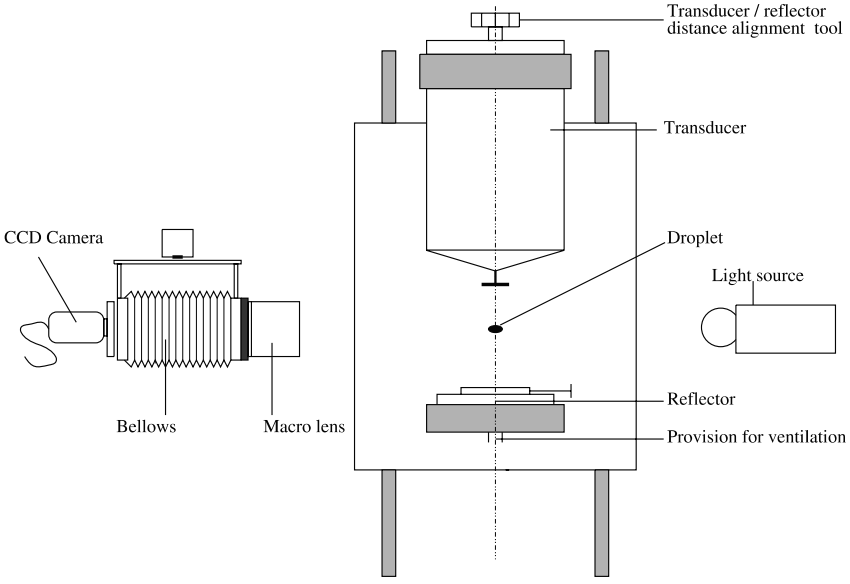

Fig. 2. Setup with the acoustic levitator used for the present droplet evaporation experiments.

content in the ambient air, given as the ratio of the partial pressure of the water vapour and the partial pressure in the state of saturation for the given temperature. To achieve the controlled environment, the acrylic glass box was ventilated with dried air. Air from the i*n*-house pressure line was dehumidified by passing it through a Calcium sulfate cartridge supplied by *Sigma Aldrich*, *Germany*. This also provides a coarse cleaning of air from particulate and other contaminations. This process was followed by sending the air into the acoustic chamber via a mass flow controller provided by *Bronkhorst*, which allows a desired flow rate of air to be set. The level of relative humidity was monitored simultaneously using a humidity sensor (*Rotronic, series I 200*).

The droplet was introduced into the acoustic pressure field using a microliter syringe. The quantity of liquid to be tested was taken into the syringe and introduced into the standing wave, thereby levitating the droplet. Initial droplet volumes of the order of 2 μl were investigated. The levitated droplet was back lighted by a white light source. A sharp image of the shadow of the ellipsoidal droplet was obtained through a CCD camera (*Tokyo Electronic Industry*, *Japan*). The CCD camera had a resolution of 752×582 pixels, and it was used with a macro lens (*Tamron SP*, *90 mm*, *1:2.5*), fixed with a bellows (Fig. 2). Details on the interactions of the levitated droplet with the ultrasound field, and the droplet evaporation in the acoustic field, are well documented in the existing literature, e.g. [13,26].

The images were processed with the software OPTIMAS. The set of information about the droplet consists of the volume-equivalent diameter, the aspect ratio of its shape, and the coordinates of the centre of gravity of the droplet with respect to some reference point in space. These data were obtained as functions of time through the software in the course of the evaporation process. Information regarding the evolution of the droplet, such as volume and surface decay, and the vertical displacement due to the mass loss, were processed as functions of time from these raw data. Experimental data were acquired at a frequency between 0.1 and 0.2 Hz, which is set through the macro in the software, depending on the volatility of the liquids investigated. The experiments for a given liquid, initial drop diameter, and liquid composition were repeated five times. The measured data for each instant of time are represented by both the average values and the rms fluctuations in the diagrams shown in the following sections. Evaporation experiments were carried out for several liquids, starting from a simple pure liquid, to complex multi-component systems. In the present paper we show the data from the multi-component liquids only.

4. Model validation

Our computational model developed on the basis of the Abramzon and Sirignano approach [7] was validated with experiments on droplets with more than two liquid components. The accuracy of a measurement was assessed by repeating the experiments and plotting the root-mean-square fluctuations of the normalised drop surface as error bars. Data on the evaporation behaviour of liquid droplets containing three, four and five liquid components are presented here. The important physico-chemical properties of the liquids investigated are presented in Table 1. The diffusion coefficients of the vapours in air are given there for the temperature $T = 293.15$ K and the pressure of 1 bar. The boiling temperatures are given for $p = 1.01325$ bar. Both properties of these liquids, which are strong functions of temperature, vary according to the homologous series they belong to. The binary diffusion coefficient, however, is the smallest for high-molecular substances, here *n*-decane (alkane) and 1-butanol (alcohol). The evaporation phenomena can be explained based on the properties pertaining to the homologous series.

The computational results are validated against the experimentally observed evolution of the normalised droplet surface and the life times of various multi-component droplets. Initial compositions are given in volume percent of the components. In Figs. 3 and 4, the surface decays of droplets of the two quaternary mixtures of methanol, ethanol, 1-butanol, *n*-heptane and water, methanol, ethanol, 1-butanol at given initial compositions are depicted. Furthermore, the evaporation behaviour of five-component droplets containing methanol, ethanol, 1-butanol, *n*-heptane, *n*-decane at two different initial compositions was investigated, and the computed evolutions of their normalised surfaces with time were compared with experimental data. The results from experiment and computation are presented in Figs. 5 and 6. All experimental data reveal a very high repeatability and also an excellent agreement with the computational results.

One issue of big interest in drop evaporation in technical processes is the life time of the droplets. A compar-

Table 1
Physico-chemical properties of the liquids investigated. Diffusion coefficients of the vapour phase in air at $p = 1$ bar and $T = 293.15$ K, boiling temperatures and latent heats of evaporation at $p = 1.01325$ bar, densities at 293.15 K

Component	Water	Methanol	Ethanol	1-Butanol	*n*-Heptane	*n*-Decane
Diffusion coefficient [cm^2/s]	0.2466	0.1573	0.1200	0.0874	0.0686	0.0567
Boiling temperature [K]	373.15	337.85	351.55	390.65	371.55	447.25
Latent heat of evaporation [kJ/kg]	2256.5	1101.0	839.0	583.0	318.0	278.0
Density [kg/m^3]	997.6	792.9	788.5	809.0	685.0	732.0
Molar mass [kg/kmol]	18	32	54	74	100	142

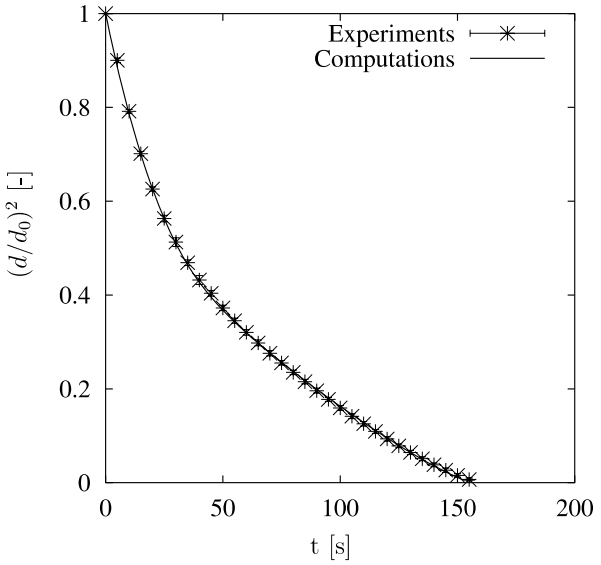

Fig. 3. Evaporation of four-component droplets with $d_0 \approx 1.57$ mm containing initially 20% methanol, 30% ethanol, 30% 1-butanol, and 20% *n*-heptane by volume at an ambient air temperature of 28 °C and a relative humidity of 3%.

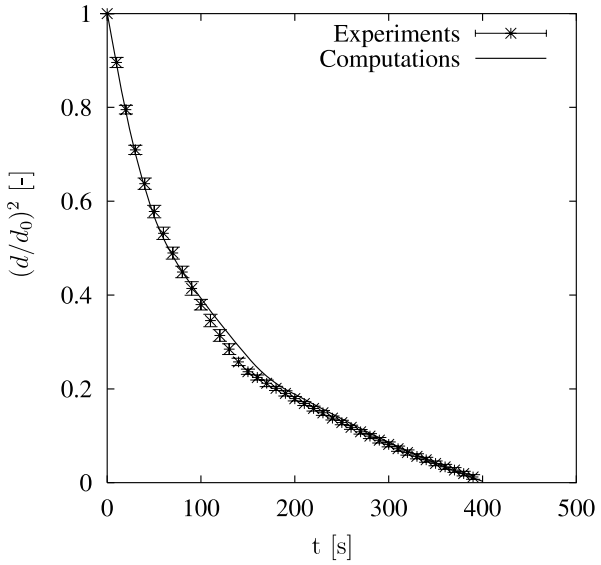

Fig. 5. Evaporation of five-component droplets with $d_0 \approx 1.72$ mm containing initially 20% by volume of methanol, ethanol, 1-butanol, *n*-heptane, and *n*-decane, at an ambient air temperature of 31 °C and a relative humidity of 2%.

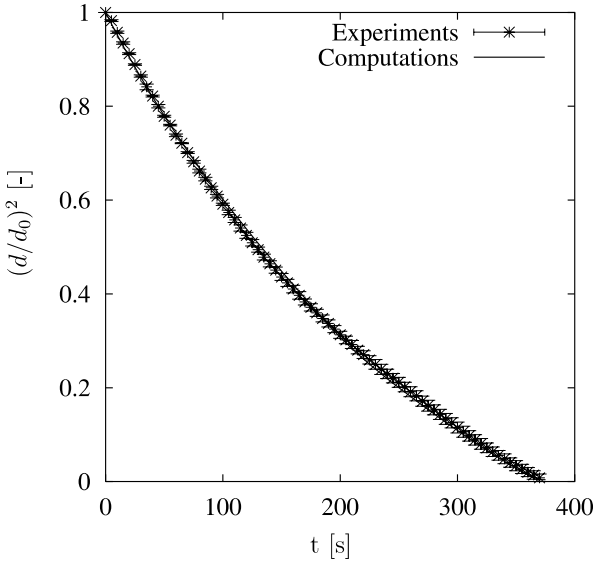

Fig. 4. Evaporation of four-component droplets with $d_0 \approx 1.5$ mm containing initially 25% by volume of water, methanol, ethanol, and 1-butanol at an ambient air temperature of ≈26 °C and a relative humidity of 2%.

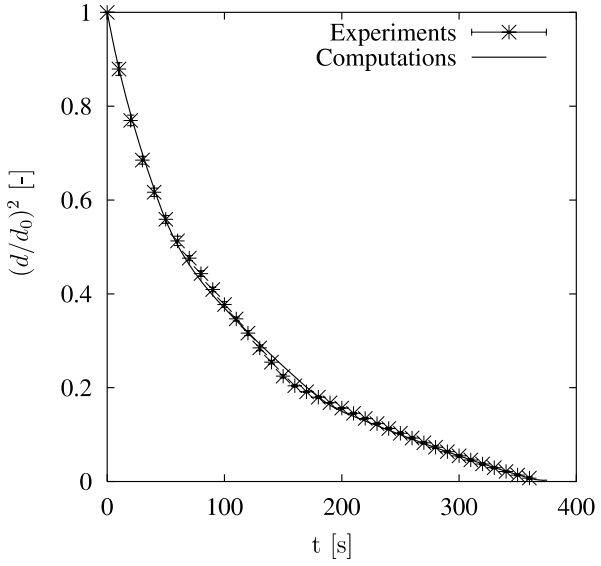

Fig. 6. Evaporation of five-component droplets with $d_0 \approx 1.72$ mm containing initially 30% methanol, 20% ethanol, 20% 1-butanol, 15% *n*-heptane, and 15% *n*-decane by volume at an ambient air temperature of 31 °C and a relative humidity of 2%.

ison of the life times of various three- and five-component droplets with different initial volume fractions of methanol, ethanol, 1-butanol, *n*-heptane and *n*-decane is shown in Fig. 7. The computed and measured life times agree very well for both the relatively simple ternary mixtures and for the more complex cases of the five-component liquids. In the whole range of values we see deviations of not more than 5%, which is an excellent result.

These comparisons clearly indicate that the model correctly represents the physico-chemical behaviour of the liquid mixtures during the evaporation process. We can therefore conclude that various phenomena, e.g. the evaporation rates of all the species present in the droplet and the evolutions of the mole fractions of the components, which cannot be easily measured, can be computed using our model. Further computed results in comparison with experimental data are presented in the following section.

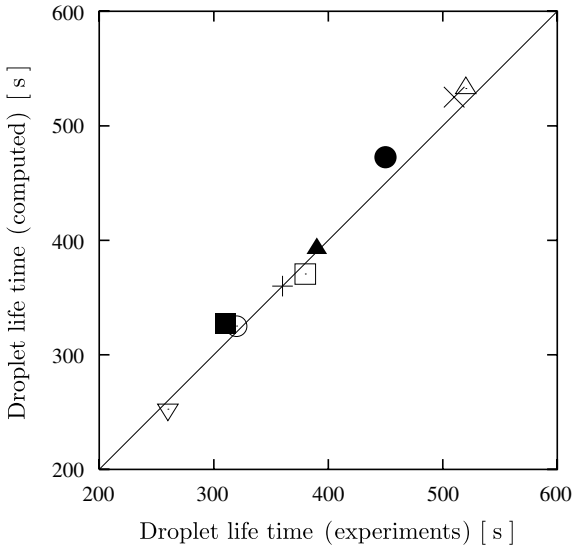

Fig. 7. Comparison of computed and measured life times of three- and five-component liquid droplets; the various symbols represent the following initial compositions of the droplet liquid: (△)10% methanol, 40% ethanol and 50% 1-butanol; (×) 30% methanol, 20% ethanol and 50% 1-butanol; (●) 10% methanol, 50% ethanol and 40% *n*-decane; ⊡ 20% methanol, 50% ethanol and 30% *n*-decane; (■) 30% methanol, 50% ethanol and 20% *n*-decane; (+) 30% methanol, 20% ethanol, 20% 1-butanol, 15% *n*-heptane and 15% *n*-decane; (⊙) 30% methanol, 30% ethanol, 10% 1-butanol, 20% *n*-heptane and 10% *n*-decane; (▽) 20% methanol, 10% ethanol, 10% 1-butanol, 40% *n*-heptane and 20% *n*-decane; (▲) 20% methanol, 20% ethanol, 20% 1-butanol, 20% *n*-heptane and 20% *n*-decane (percentages by volume).

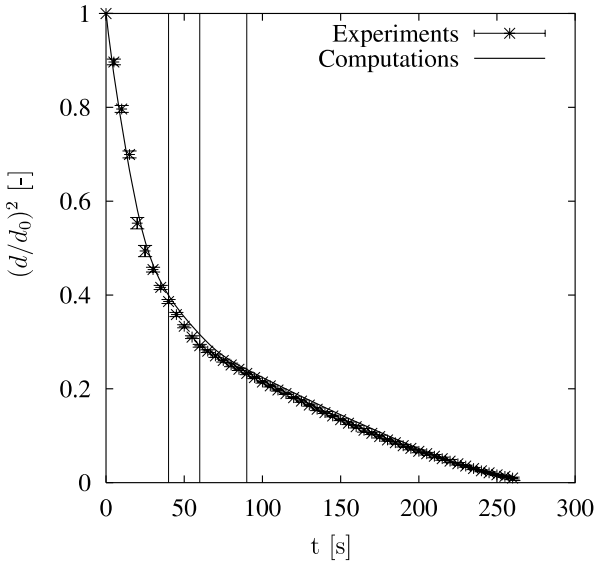

Fig. 8. Evaporation of five-component droplets with $d_0 \approx 1.5$ mm containing initially 20% methanol, 10% ethanol, 10% 1-butanol, 40% *n*-heptane, and 20% *n*-decane by volume at an ambient air temperature of 28 °C and a relative humidity of 3%.

5. Detailed analysis of multi-component liquid droplet evaporation

In the present section we analyze the evaporation behaviour of five-component liquid droplets at varying initial composition. The five components are three alcohols (methanol, ethanol and 1-butanol) and two alkanes (*n*-heptane and *n*-decane), mixed at varying initial volume fractions. Water is not a component of these mixtures, since it is immiscible with the alkanes.

A droplet of 1.50 mm initial diameter containing initially 20% by volume of methanol, 10% ethanol, 10% 1-butanol, 40% *n*-heptane, and 20% *n*-decane is levitated in a controlled environment with a relative humidity of 3% at an air temperature of 301.15 K.

Fig. 8 shows the evolution of the normalised surface with time. The curve clearly exhibits the presence of various slopes in the evolution of the normalised surface, which represent the influence of various components with different volatilities. In the present case four distinct slopes are visible, which mark the evaporation of various components (starting from the highly volatile substances and going to the least volatile ones). The evolutions of the mole fractions of the components in the liquid phase for the initial liquid composition of Fig. 8 are illustrated in Fig. 9. The mole fractions of the various components *i* were calculated as

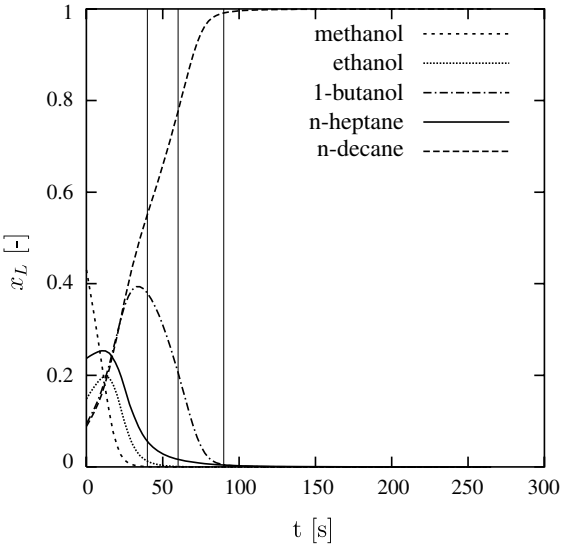

Fig. 9. Mole fraction evolution of five-component droplets with $d_0 \approx 1.5$ mm containing initially 20% methanol, 10% ethanol, 10% 1-butanol, 40% *n*-heptane and 20% *n*-decane by volume at an ambient air temperature of 28 °C and a relative humidity of 3%.

$$x_i = \frac{(\rho_i/M_i)\varphi_i}{\sum_j (\rho_j/M_j)\varphi_j}, \tag{30}$$

where M_i and φ_i are the molar mass and the volume fraction of component *i*, respectively. Many interesting features of evaporating multi-component droplets can be deduced from this figure. It is evident that the content of the most volatile substance methanol decays quickly, which is represented by the first slope in the evolution of the normalised drop surface. The evaporation of ethanol dominates the

second slope. In the mole fraction graph in Fig. 9, the mole fraction of the next volatile component, 1-butanol, reaches its maximum as the mole fraction of methanol decreases to zero. The various stages of evaporation are indicated by the three vertical lines in Figs. 8 and 9, which mark the approximate times where – from left to right – methanol, ethanol, and *n*-heptane as well as 1-butanol have disappeared from the droplet. From the time $t \approx 115$ s on, the droplet is left with *n*-decane only, which is illustrated by the mole fraction of 1.0 of this component. The total life time of this droplet is 264 s.

The temporal evolution of the droplet temperature calculated with our model for various five-component mixtures is shown in Fig. 10. The complexity in the evolution of the droplet temperature with time is not surprising. Although we do not account for the mixing enthalpy of the components, some conclusions can nevertheless be drawn from Fig. 10. At the beginning of the evaporation process, the temperatures of all the mixtures, except system 1, decrease until a wet-bulb temperature of the mixtures dominated by methanol is reached. The following temperature increase is relatively steep for system 4, which is due to the low content of more volatile and the high content of less volatile components. At the end of the droplet life the only remaining component, the least volatile one, evaporates at constant droplet temperature. System 4 exhibits the lowest final temperature due to its special composition. It should be mentioned that the data in Fig. 10 were computed to simulate various droplet evaporation experiments, which were carried out at different ambient air temperatures and relative humidities. This is the reason for the slightly different temperatures in the final states of the droplets seen in the figure.

Having established the connection between the properties of the substances used and the homologous series as outlined above, it is interesting to examine various aspects of multi-component droplet evaporation. Fig. 11 depicts the computed surface decays of five-component droplets. This plot not only conveys information about the variation of the droplet surface, but also on the variation of the droplet life time with varying initial composition. As seen in Fig. 11, the life times of multi-component droplets containing the same components at varying initial volume fractions vary considerably. The present analysis shows an increase in the life time of about 54% when the volume fraction of the highly volatile component *n*-heptane is reduced by 50%. The surface decay profiles of the droplets investigated are virtually identical for systems 1, 2, and 3. A slight difference in the slopes of system 4 is due to the relatively high content of *n*-heptane in the droplet.

Fig. 12 depicts the computed surface decays of the five-component droplets in Fig. 11 as functions of the Fourier number for mass transfer

$$Fo = \frac{D_{\min} t}{d_0^2}. \tag{31}$$

This abscissa variable differs from the often used variable t/d_0^2 [6,29] in that it is non-dimensional, but it exhibits the same scaling properties as the latter, since the diffusion

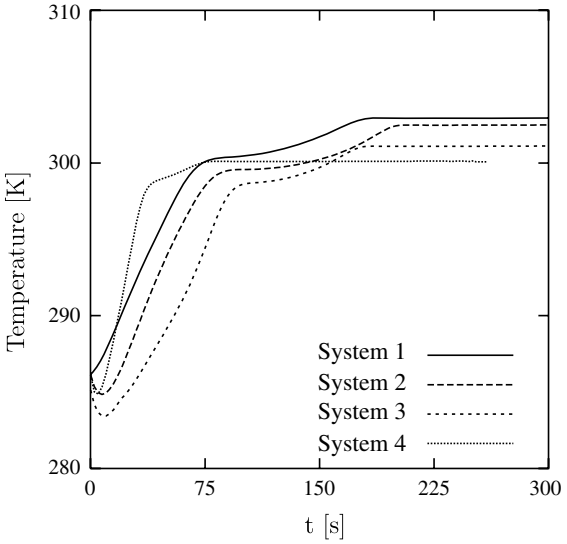

Fig. 10. Temperatures of five-component liquid droplets as functions of time; initial liquid compositions (with the ambient air temperatures and relative humidities): system 1 – 20% methanol, 20% ethanol, 20% 1-butanol, 20% *n*-heptane and 20% *n*-decane (31 °C, 2%); system 2 – 30% methanol, 20% ethanol, 20% 1-butanol, 15% *n*-heptane and 15% *n*-decane (30 °C, 2%); system 3 – 30% methanol, 30% ethanol, 10% 1-butanol, 20% *n*-heptane and 10% *n*-decane (29 °C, 3%); system 4 – 20% methanol, 10% ethanol, 10% 1-butanol, 40% *n*-heptane and 20% *n*-decane (29 °C, 3%) (percentages of component contents by volume).

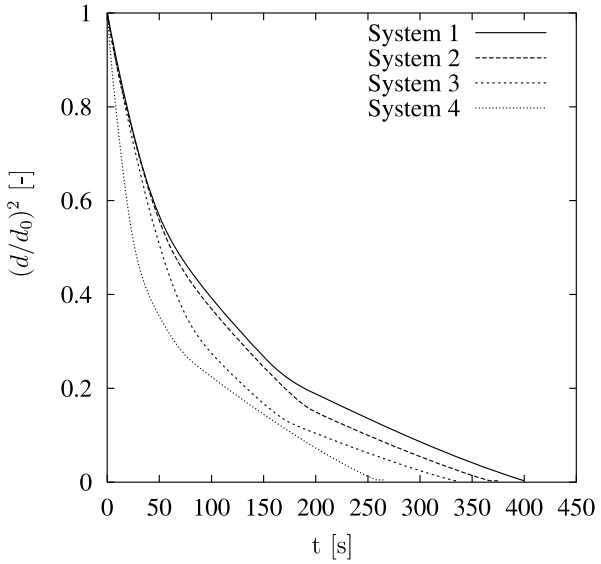

Fig. 11. Influence of the initial composition on five-component droplet life time; initial liquid compositions (with the ambient air temperatures and relative humidities): system 1 – 20% methanol, 20% ethanol, 20% 1-butanol, 20% *n*-heptane and 20% *n*-decane (31 °C, 2%); system 2 – 30% methanol, 20% ethanol, 20% 1-butanol, 15% *n*-heptane and 15% *n*-decane (30 °C, 2%); system 3 – 30% methanol, 30% ethanol, 10% 1-butanol, 20% *n*-heptane and 10% *n*-decane (29 °C, 3%); system 4 – 20% methanol, 10% ethanol, 10% 1-butanol, 40% *n*-heptane and 20% *n*-decane (29 °C, 3%) (percentages of component contents by volume).

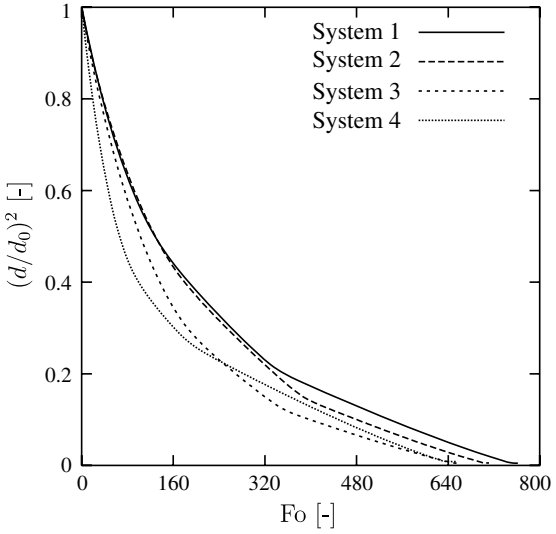

Fig. 12. Influence of the initial composition on five-component droplet life time as a function of the Fourier number; initial liquid compositions (with the ambient air temperatures and relative humidities): system 1 – 20% methanol, 20% ethanol, 20% 1-butanol, 20% *n*-heptane and 20% *n*-decane (31 °C, 2%); system 2 – 30% methanol, 20% ethanol, 20% 1-butanol, 15% *n*-heptane and 15% *n*-decane (30 °C, 2%); system 3 – 30% methanol, 30% ethanol, 10% 1-butanol, 20% *n*-heptane and 10% *n*-decane (29 °C, 3%); system 4 – 20% methanol, 10% ethanol, 10% 1-butanol, 40% *n*-heptane and 20% *n*-decane (29 °C, 3%) (percentages of component contents by volume).

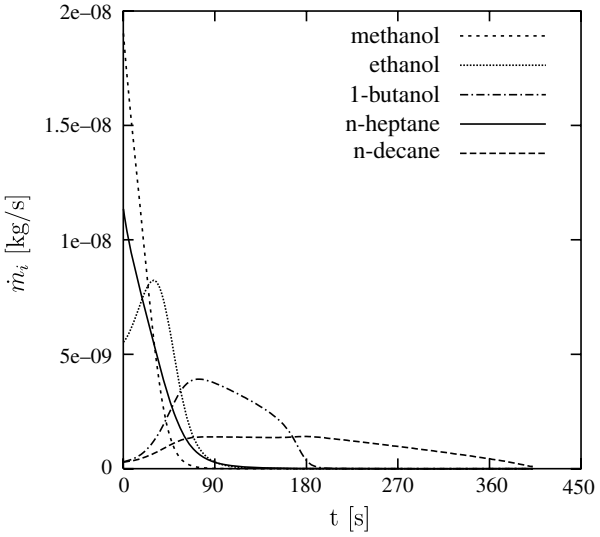

Fig. 13. Temporal evolution of the evaporation rates $\dot{m}_i$ of the mixture components of droplets with $d_0 \approx 1.72$ mm containing initially 20% methanol, 20% ethanol, 20% 1-butanol, 20% *n*-heptane, and 20% *n*-decane by volume at an ambient air temperature of 31 °C and a relative humidity of 3%.

coefficient $D_{\min}$ is just a constant factor with a dimension to render the scaled time t/d_0^2 non-dimensional. For the present representation of data, the diffusion coefficient of *n*-decane vapour in air was used as $D_{\min}$. The Fourier number represents the ratio of elapsed time to the characteristic diffusion time scale. In Fig. 12 the beginning of the surface decay curves hardly differs from the dimensional representation in Fig. 11, but there can be clearly seen a difference at the end of the evaporation process. The curves for systems 3 and 4 nearly reach an equal final Fourier number, and the final values of *Fo* for systems 1 and 2 are also nearly equal, but different from the first mentioned one. Thus, the particular behaviour of system 4 cannot be observed here any more due to the different scaling of the non-dimensional time as the abscissa variable.

Though it is difficult to predict the interaction between the components, quantitative results, such as the mole fraction evolution inside a droplet, the evaporation rate of individual components of the liquid mixture, and the instantaneous evaporation rate of the multi-component droplet can be obtained from the computations. Fig. 13 shows the computed temporal evolutions of the individual evaporation rates of the components of a five-component liquid mixture. It is evident from this figure that the evaporation rates of methanol and *n*-heptane start with a high value and decrease rapidly without reaching another maximum, whereas the other component evaporation rates exhibit a maximum during the droplet life time. The evaporation rate of *n*-decane is almost constant for a time period between 75 and 185 s, suggesting that this liquid is not very susceptible to any thermodynamical variations inside the liquid droplet during this period of time. However, as a consequence of depletion of the other components from the liquid droplet, the evaporation rate of *n*-decane decreases after 185 s.

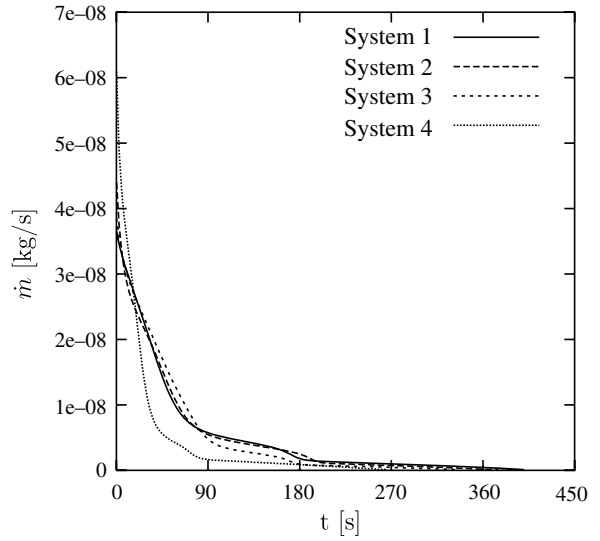

Fig. 14. Influence of the initial composition on the temporal evolution of the evaporation rate of multi-component droplets; initial liquid compositions (with the ambient air temperatures and relative humidities): system 1 – 20% methanol, 20% ethanol, 20% 1-butanol, 20% *n*-heptane and 20% *n*-decane (31 °C, 2%); system 2 – 30% methanol, 20% ethanol, 20% 1-butanol, 15% *n*-heptane and 15% *n*-decane (30 °C, 2%); system 3 – 30% methanol, 30% ethanol, 10% 1-butanol, 20% *n*-heptane and 10% *n*-decane (29 °C, 3%); system 4 – 20% methanol, 10% ethanol, 10% 1-butanol, 40% *n*-heptane and 20% *n*-decane (29 °C, 3%) (percentages of component contents by volume).

For an estimation of the total rate of mass transfer from evaporating multi-component droplets, the total evaporation rate of the liquid mixture as the sum of all component evaporation rates is needed as a function of time. The total evaporation rate of four different five-component droplets is depicted in Fig. 14. The data represent the behaviour of the four systems shown in Figs. 11 and 12 already. It can be seen that the evolutions for systems 1 to 3 are almost the same, whereas system 4 clearly shows a lower value during most of the time. Again this is due to its special composition (more low volatile, less high volatile components). We see a steep decrease of the total evaporation rate of the droplet within the first 90 s of the droplet lifetime down to a very low value, which remains constant for most of the remaining 160 s of droplet life.

6. Conclusions

A computational model for the simulation of the evaporation behaviour of multi-component liquid droplets was developed and validated experimentally. The model is based on the model of pure liquid droplet evaporation by Abramzon and Sirignano and extends that model to multi-component liquid mixtures. The essential issue is the mutual influence of the various liquid components affecting their activities, which is modelled using the UNIFAC approach. Mixing enthalpy is not accounted for. The model is not limited in terms of the number of components in the liquid phase. Verification experiments were carried out with ultrasonically levitated single liquid droplets consisting of up to five components. Computational and experimental results on the decay of the droplet surface with time agree very well, indicating that the model represents the relevant physico-chemical phenomena in multi-component liquid evaporation correctly. The special kind of forced convective transport situation in the acoustic levitator does not imply a limitation to the validity of our model. Any convective transport, caused by relative motion of a gas and a droplet, quantified by the *Re*, *Pr*, and *Sc* numbers, may be simulated using our approach.

The maximum deviation of measured and computed lifetimes of the droplets of various multi-component mixtures of 5% is an excellent result. From the computed data, rates of evaporation of the various components and the evolutions of component concentrations and droplet temperature with time can be deduced. This kind of information cannot be readily obtained from the levitator experiments, which consist predominantly in geometrical information. The model validated at laboratory temperature and atmospheric air pressure may be used within the range of temperatures and pressures applicable with the Abramzon and Sirignano and UNIFAC models.

Acknowledgements

The present work was carried out at the Chair of Fluid Mechanics (LSTM) of the University of Erlangen-Nürnberg in the frame of the research project "DIME – Direct injection engine spray processes. Mechanisms to improve performance" of the European Union. Financial support from the European Commission under contract number ENK6-CT-2000-00101 is gratefully acknowledged. Part of the mathematical modelling was carried out by C. Fink in the work for his diploma thesis. We acknowledge the contributions to his supervision from Mr. E. v. Berg at AVL Graz.

References

[1] F.R. Newbold, N.R. Amundson, A model for evaporation of a multicomponent droplet, AIChE J. 19 (1973) 22–30.
[2] D.A. Frank-Kamenetzki, Diffusion and Heat Transfer in Chemical Kinetics, second ed., Plenum Press, New York, 1969.
[3] J. Abraham, V. Magi, A model for multi-component droplet vaporization in sprays, SAE Technical paper 980511, 1998, pp. 117–127.
[4] C.K. Law, H.K. Law, A d^2-law for multicomponent droplet vaporization and combustion, AIAA J. 20 (1982) 522–527.
[5] R. Kneer, M. Schneider, B. Noll, S. Wittig, Diffusion controlled evaporation of a multicomponent droplet: theoretical studies on the importance of the variable liquid properties, Int. J. Heat Mass Transfer 36 (1993) 2402–2415.
[6] A.J. Marchese, F.L. Dryer, The effect of liquid mass transport on the combustion and extinction of bicomponent droplets of methanol and water, Combust. Flame 105 (1996) 104–122.
[7] B. Abramzon, W.A. Sirignano, Approximate theory of a single droplet vaporization in a convective field: effects of variable properties, Stefan flow and transient liquid heating, in: Proc. 2nd ASME–JSME Thermal Engng. Joint Conf., Hawaii, vol. 1, 1987, pp. 11–18.
[8] R.B. Bird, W.E. Stewart, E.N. Lightfoot, Transport Phenomena, John Wiley and Sons, New York, 1960.
[9] O. Kastner, Theoretische und experimentelle Untersuchungen zum Stoffübergang von Einzeltropfen in einem akustischen Rohrlevitator, PhD thesis, Friedrich-Alexander University of Erlangen-Nürnberg, Germany, 2001.
[10] R. Kneer, Grundlegende Untersuchungen zur Sprühstrahlausbreitung in hochbelasteten Brennräumen: Tropfenverdunstung und Sprühstrahlausbreitung, PhD thesis, University of Karlsruhe, Germany, 1996.
[11] N. Frössling, Über die Verdunstung fallender Tropfen, Gerlands Beitr. z. Geophysik 52 (1938) 170–216.
[12] W.E. Ranz, W.R. Marshall, Evaporation of drops – Part 1, Chem. Eng. Progr. 48 (1954) 141–146.
[13] A.L. Yarin, G. Brenn, O. Kastner, D. Rensink, C. Tropea, Evaporation of acoustically levitated droplets, J. Fluid Mech. 399 (1999) 151–204.
[14] E.G. Lierke, Akustische Positionierung - ein umfassender Überblick über Grundlagen und Anwendungen, Acta Acustica 82 (1996) 220–237.
[15] P.L. Marston, S.E. LoPorto-Arione, G.L. Pullen, Quadrupole projection of the radiation pressure on a compressible sphere, J. Acoust. Soc. Am. 69 (1981) 1499–1501.
[16] A. Gopinath, A.F. Mills, Convective heat transfer from a sphere due to acoustic streaming, Trans. ASME – J. Heat Transfer 115 (1993) 332–341.
[17] G. Brenn, L.J. Deviprasath, F. Durst, Computations and experiments on the evaporation of multicomponent droplets, in: Proc. 9th Int. Conf. Liquid Atomiz. Spray Systems (ICLASS), Sorrento (Italy), July 13–17, 2003.
[18] G. Brenn, Concentration fields in evaporating droplets, Int. J. Heat Mass Transfer 48 (2005) 395–402.
[19] R.C. Reid, J.M. Prausnitz, T.K. Sherwood, The Properties of Gases and Liquids, third ed., McGraw Hill, New York, 1977.

[20] M. Hirata, S. Ohe, K. Nagahama, Computer-aided book of vapor–liquid equilibria, Elsevier, Amsterdam, 1975.
[21] J. Gmehling, P. Rasmussen, Aa. Fredenslund, Vapor–liquid equilibria by UNIFAC group contribution. Revision and extension 2, Ind. Eng. Chem. Process Des. Dev. 21 (1982) 118–127.
[22] J.M. Prausnitz, J. Gmehling, Thermische Verfahrenstechnik – Phasengleichgewichte, Krausskopf, Mainz, 1980.
[23] J.A. Zarkarian, F.E. Anderson, J.A. Boyd, J.M. Prausnitz, UNIFAC parameters from gas–liquid chromatographic data, Ind. Eng. Chem. Process Des. Dev. 18 (1979) 657–661.
[24] VDI – Verein Deutscher Ingenieure (Association of German Engineers) (Eds.) – VDI Wärmeatlas, 9th ed. Springer, Berlin, 2002.
[25] Aa. Fredenslund, R.M. Jones, J.M. Prausnitz, Supplement to program UNIFAC – Group contribution estimation of activity coefficients in nonideal liquid mixtures, report University of California, Berkeley CA (USA), 5th revision 1992.
[26] A.L. Yarin, M. Pfaffenlehner, C. Tropea, On the acoustic levitation of droplets, J. Fluid Mech. 356 (1998) 65–91.
[27] E. Welter, B. Neidhart, Acoustically levitated droplets – a new tool for micro and trace analysis, Fres. J. Anal. Chem. 357 (1997) 345–350.
[28] M. Petersson, J. Nilsson, L. Wallman, T. Laurell, J. Johansson, S. Nilsson, Sample enrichments in a single levitated droplet for capillary electrophoresis, J. Chromatogr. B 714 (1998) 39–46.
[29] H. Nomura, Y. Ujiie, H.J. Rath, J. Sato, M. Kono, Experimental study on high-pressure droplet evaporation using microgravity conditions, in: Proc Twenty-Sixth Int. Symp. Combustion, The Combustion Institute, 1996, pp. 1267–1273.